

Influence of carbon and phosphorus doping on electronic properties of ZnO

Vidhika Sharma^{1,3} · Mohit Prasad² · Sandesh Jadkar³ · Sourav Pal^{1,4}

Received: 15 March 2016 / Accepted: 13 June 2016 / Published online: 22 June 2016
© Springer Science+Business Media New York 2016

Abstract ZnO is one of the most promising candidate for photoelectrochemical splitting of water for hydrogen production. To increase the efficiency of ZnO based photoelectrochemical cell, its band-gap and band edges should be tailored to match visible light spectra and water redox potential respectively. In this paper, First-principles density functional theory calculations have been performed to evaluate the effect of non-metal dopants on electronic properties of ZnO. The model structures of X-doped ZnO were constructed using 32-atom $2 \times 2 \times 2$ supercell of wurtzite ZnO with one O atom replaced with X (carbon C, phosphorus P). With respect to the electronic band structure, C ($2p$), P ($3p$) states are located above the valence band maximum of ZnO and mixing of these states is feeble to produce significant band gap narrowing. Doping of these non-metals dopants helps in the creation of isolated states which enhances visible light absorption of ZnO. Our theoretical calculations are consistent with the experimental results of C (P) doped ZnO and fully explains its visible light activity on non-metal doping.

1 Introduction

The ever increasing demand of energy in every sphere of human activity, dwindling fossil fuel reserves and threat of climate change has forced everyone to look for alternative renewable energy sources. Solar produced hydrogen is envisioned as an ideal energy carrier and fuel for the future [1, 2]. Photoelectrochemical (PEC) water splitting is the “holy grail” for clean and green hydrogen production. Since the pioneering work of Fujishima and Honda in 1972, who demonstrated that overall water splitting can be achieved in a PEC cell consisting of single crystalline TiO_2 anode and a Pt cathode under UV irradiation assisted by an electric bias, extensive work has been taken up by researchers around the world [3]. The concept of this technique is based on a semiconductor photoelectrode device that excites with sunlight, oxidizes/reduces H_2O molecules by h^+/e^- pair and transforms it to chemical energy (i.e. H_2 gas). In order to have an efficient PEC reaction, the chosen semiconductor must have a few significant properties such as: suitable band gap and band edges position, high charge carrier mobility and chemical stability [4].

ZnO is the most coveted semiconductor as it has strong photocatalytic activity, high electron mobility, nontoxic nature, well aligned band edges, high exciton binding energy (60 meV), high cohesion and extraction ability making it one of the most promising photocatalyst for hydrogen production through PEC splitting of water. It has shown applications in diverse fields such as ultrahigh band width microwave absorbers [5], flexible ceramics [6, 7] gas sensors [8], photodetectors [9], and in photocatalysis [10]. However, a high intrinsic band gap of ZnO (3.2 eV) allows absorption of only UV light which correspond to 4 % of solar spectrum [11]. Various attempts are in progress to

✉ Vidhika Sharma
vidhika15@gmail.com

✉ Sandesh Jadkar
sandesh@physics.unipune.ac.in

¹ Electronic Structure Theory Group, Physical and Material Chemistry Division, CSIR-National Chemical Laboratory, Pune 411 008, India

² Department of Physics, SKN-Sinhgad Institute of Technology and Science, Lonavala, Kusgaon 410 401, India

³ Department of Physics, Savitribai Phule Pune University, Pune 411 007, India

⁴ Department of Chemistry, Indian Institute of Technology Bombay, Powai, Mumbai 400 076, India

solve this problem that would enhance the PEC performance of ZnO photoanodes [12–15]. In the past few years, impurity doping has been investigated vigorously as a method to extend the absorption spectrum of ZnO in visible region. Instead of cationic doping in ZnO, anionic doping had resulted in high level of photoactivity under visible light irradiation [16–22]. For instance, Yang et al. [16] found that the visible light PEC activity of N-doped ZnO is about 3.5 times higher than the activity of pure ZnO. Liu et al. [21] have synthesized a flower like C doped superstructure exhibiting enhanced photocatalytic activity which can be attributed to the effect of C doping into the ZnO lattice. The optical property of P doped ZnO has also been experimentally investigated by some groups [22]. The microscopic mechanism underlying this phenomenon has not been fully explored yet. To the best of our knowledge, the changes in the electronic band structures of C (P) doped ZnO has not been extensively investigated with respect to solar energy.

In this paper, we present the first-principles spin-polarized calculations of electronic band structures of C (P) doped ZnO. A systematic quantum chemical calculation using density functional theory (DFT) has been presented, which describes and explains the effect of individual non-metal (C, P) dopant elements on the electronic structure of ZnO. Doping C (P) atoms in appropriate position of ZnO lattice is able to alter both geometric and electronic structures, which can primarily determine their optical properties and hence corresponding PEC activity. The obtained results show that above the top of O $2p$ valence band the substitution of O by C or P may introduce isolated states. The band-gap narrowing driven by the strong mixing of C ($2p$) or P ($3p$) with O $2p$ states is minor in nature. Our results are consistent with the experimental data [20–22]. The C ($2p$), P ($3p$) states localized above the valence-band maximum of ZnO are responsible for the absorption of visible light. The theoretical calculations provide a clear insight of the effect of mono doping and will be helpful in designing efficient photocatalysts for PEC splitting of water.

2 Details and calculations

In this study we have considered a $2 \times 2 \times 2$ supercell of a wurtzite ZnO, consisting 16 Zn atoms and 16 O atoms, as shown in Fig. 1. Mono doping model was constructed by substituting one O atom, which corresponds to the X concentration of 6.25 at.%. The properties of the defects calculated from a $2 \times 2 \times 2$ ZnO supercell such as this could be used for qualitative analysis [15].

Our first-principle calculations were performed using the Vienna ab initio Simulation Package (VASP) based on

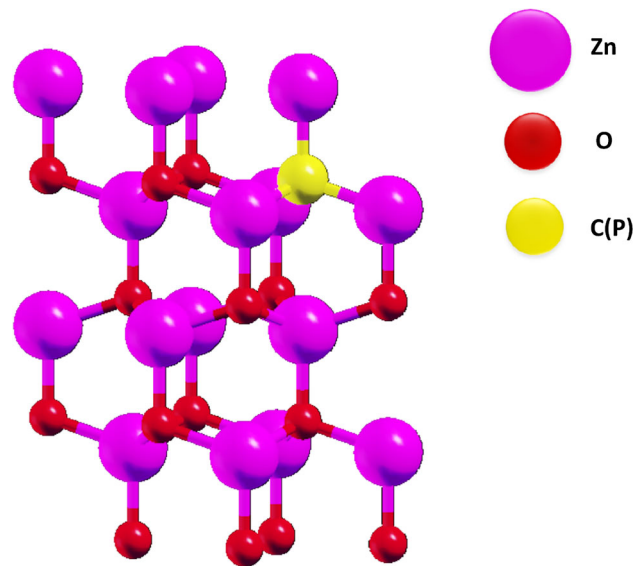


Fig. 1 Atomic representation of $2 \times 2 \times 2$ super cell of C (P)-doped ZnO

the DFT with the projected augmented wave pseudo-potentials [23]. The exchange–correlation potential is formulated by the generalised gradient approximation (GGA). Hubbard potential (U) was introduced in the calculations, to correct the energy positions of Zn ($3d$) states [24]. The value of U was taken 4.0 eV for Zn. Structural optimization was performed on each model before calculating properties. The electron wave functions were expanded in plane wave with an energy cut off of 520 eV. The energy convergence criterion for the self-consistent field was set at 10^{-6} eV. The Monkhorst–Pack scheme K point’s grid sampling in the supercell was set at $4 \times 4 \times 2$. The valence configurations of the atoms were $4s^2 3d^{10}$ for Zn, $2s^2 2p^4$ for O, $2s^2 2p^2$ for C and $3s^2 3p^3$ for P.

3 Results and discussion

To study the effect of non-metal doping on the electronic band structure of ZnO, we have first calculated the various crystal structural parameters of the pure ZnO. The optimized structural parameters of pure ZnO such as average bond-length (1.98 Å) and the lattice parameters

Table 1 Optimized structural parameters for undoped and doped ZnO

	Lattice-constant (Å)	Bond-length (Å)
Zn–O	6.58	1.98
Zn–C	6.60	2.06
Zn–P	6.62	2.24

($a = 3.28 \text{ \AA}$, $c = 5.28 \text{ \AA}$) are shown in Table 1. To investigate the effect of individual dopant elements, we have optimized the $2 \times 2 \times 2$ super-cell geometry of C (P) doped ZnO. The calculated bond-length and lattice parameters of C (P) doped ZnO are compared with the pure ZnO and are shown in Table 1. The optimized structural parameters of C (P) doped ZnO are almost analogous with pure ZnO, which confirms the stability and feasibility of these dopants in ZnO crystal. The bond length of C (P) doped ZnO slightly increases as compared to the pure ZnO. The structural variations following the replacement of one O atom with one P in the 32-atom supercell appear to be more pronounced than for C doped ZnO. This implies that the incorporation of P in ZnO yields more strain to the neighbouring Zn atoms as compared to strain induced in ZnO via C doping. The calculated values are in complete agreement with the previous published results [25, 26].

To comprehend the effect of C (P) doping on electronic structure and to explain the origin of visible light photoactivity in ZnO, both DOS and band structure were calculated based on the optimized crystal structure and are shown in Fig. 1. In order to modify the band structure of ZnO through non-metal doping we need to know the atomic wave function characteristics of the band edge states. As shown in Fig. 2a the valence band of pure ZnO mainly comprises of O $2p$, Zn $3d$ and O $2s$ states, while the conduction band is dominated by Zn $4s$, Zn $3p$ and O $2p$ states. The Fermi level was set to zero and is indicated by dotted line. The calculated value of pure ZnO band gap is 1.1 eV using GGA method with Hubbard potential, which is smaller than the experimental value (3.2 eV) due to the well-known shortcomings of GGA method [27]. Moreover, it can be seen from Fig. 2b that the conduction band minima (CBM) and valence band maxima (VBM) is located at the same symmetric gamma G (Γ) point, indicating that pure ZnO is a direct band gap semiconductor. We were mainly concerned with the change of the band gap on doping, so the absolute value of band gap was not a matter of concern. However, to modify band-gap and band edges and match with visible light spectra and water redox potential, we should upshift the VBM by incorporating dopant of different p orbital energy higher than oxygen. On the other hand, we need to maintain or raise the CBM by choosing dopant of different s, p orbital energy than O $2p$ and Zn $4s$.

We had further investigated the density of states (DOS) and PDOS of C (P) doped ZnO. The results are shown in Fig. 3. There is a small shift of O $2p$ VBM in C (P) doped ZnO with respect to pure ZnO. The electronic state of C and P contributes to the valence band of ZnO, and it comes from their $2p$ and $3p$ states, respectively. The conduction band of ZnO mainly comprises of Zn $4s$ states, thus these non-metal dopants have a little influence over the

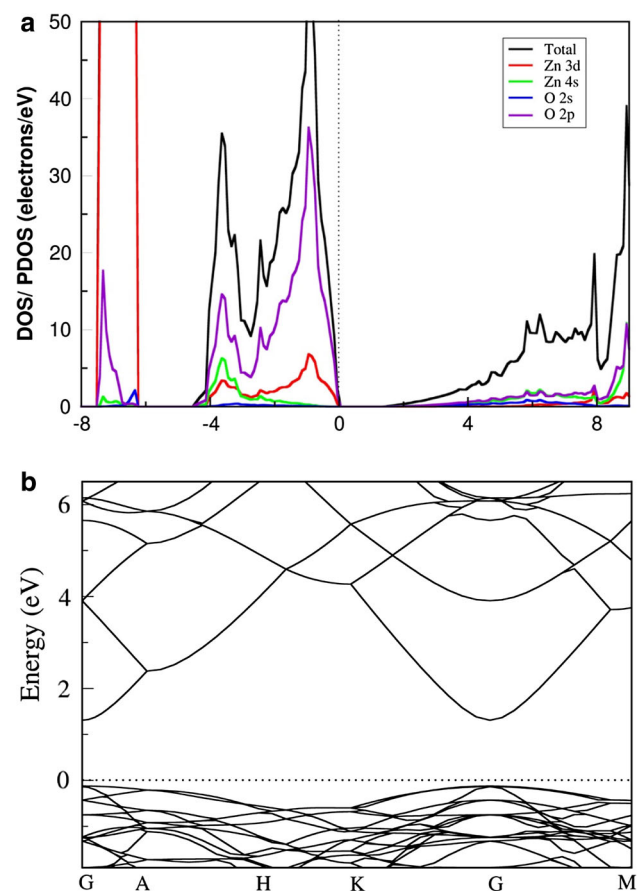


Fig. 2 Total density of states (TDOS) and electronic band structure of pure ZnO

composition of conduction band. The conduction band shifts towards the lower energy region as compared to pure ZnO. It is also evident from Fig. 4 that charge density is distributed spherically on the C (P) atoms. Then bond length of Zn–O in doped case is more than the undoped one. The interaction between the neighbouring atoms and C (P) decreases tending to break the Zn–C, Zn–P and the Zn–O bonds. This leads to the creation of holes around the dopants as the electrons become free. These holes are responsible for the formation of acceptor levels. The acceptor levels which are formed by C (P) are shallower, but they are still deep enough to attain p-type transformation [20, 28]. As clear from Fig. 3, C ($2p$) and P ($3p$) increase the total electron density at Fermi level and can also create more isolated states extending into the region above the Fermi level. This makes it easier for electron present at the Fermi level to skip into higher energy region via thermal and photo excitation by exploiting these available isolated states. As the atomic size and electro-negativity of oxygen atoms is similar to C ($2p$) and P ($3p$) states, so both are located closer to the Fermi level of the doped ZnO. Since the electronic states of C (P) doped ZnO

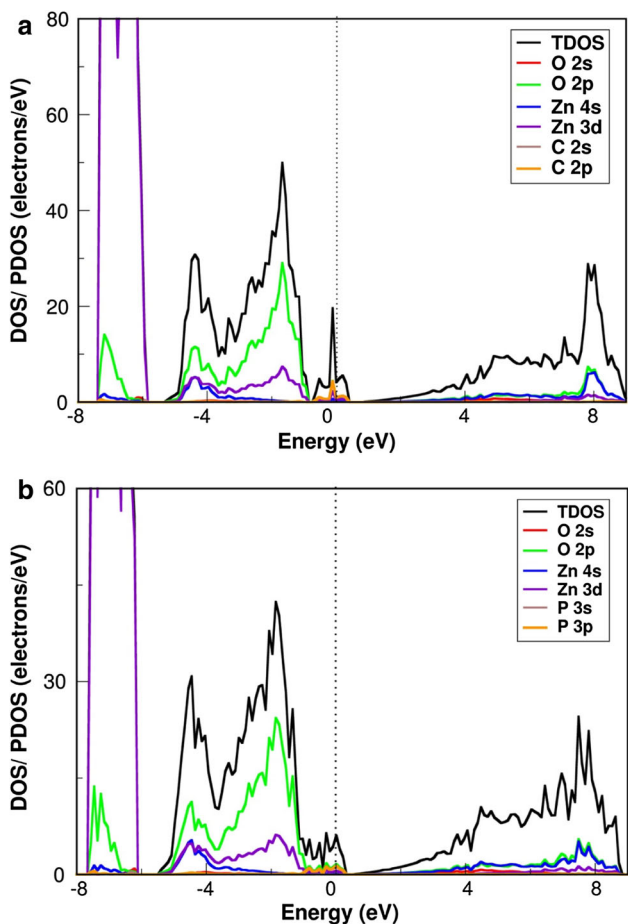


Fig. 3 Partial density of states (PDOS) of C (a) and P (b) doped ZnO

are in the vicinity of Fermi level, so it affects the physical properties, widens the absorbance range and thus enhances the PEC activity [20–22].

The calculated GGA + U band structure of C (P) doped ZnO along the high symmetry directions in the Brillouin zone is shown in Fig. 5. The VBM and CBM of C (P) doped ZnO are both located at the same high symmetric G (Γ) point, indicating direct electron transition in the band gap region confirming the experimental results [20–22].

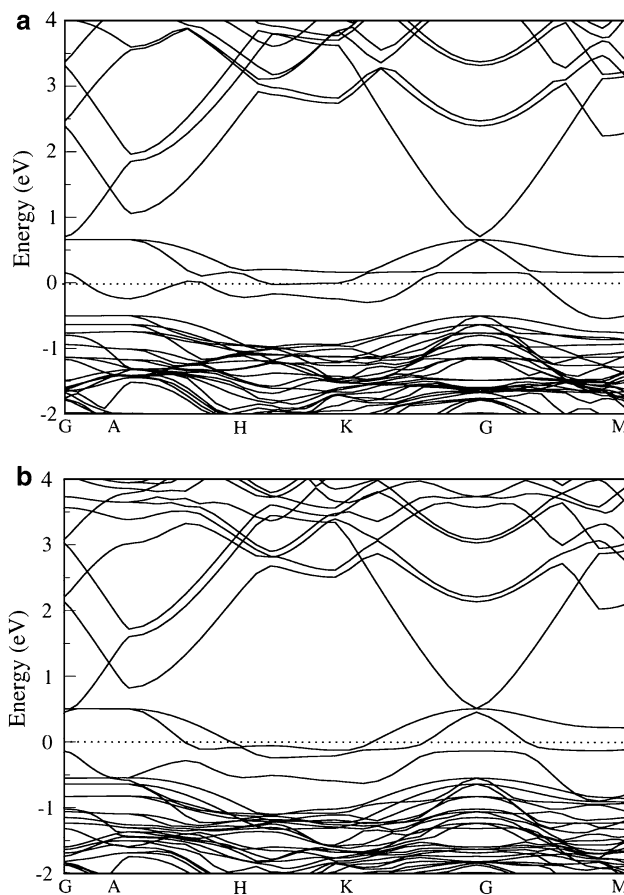
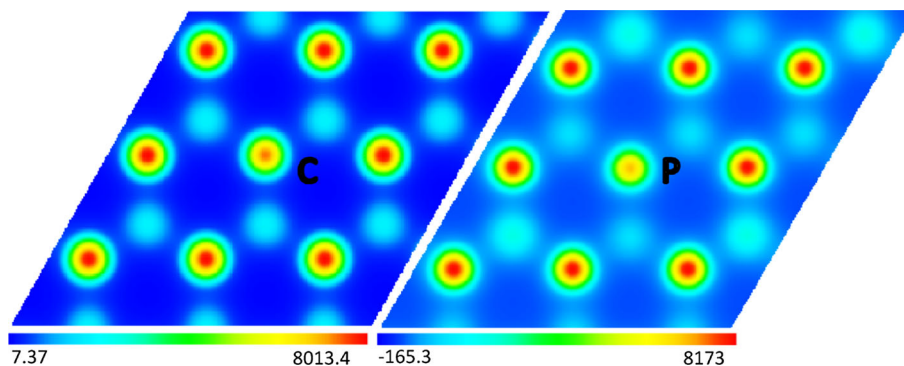


Fig. 5 Electronic band structure of C (a) and P (b) doped ZnO

Compared to pure ZnO, isolated states appear in C (P) doped ZnO above the top of the O 2p valence band at 0.4 and 0.2 eV, respectively, as shown in Fig. 5. So, we can conclude that the substitution of C (P) for O will introduce isolated impurity bands in the band gap region. These isolated states appear above the Fermi level and serves as a trampoline for electrons to jump into the conduction band by thermal and photo-excitation. This phenomenon reduces the demand of photon energy and facilitates the transfer of photogenerated electrons and holes and eventually enhances the

Fig. 4 Calculated charge density distribution of C (P)-doped ZnO



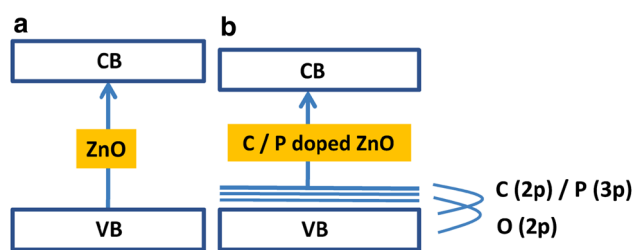


Fig. 6 Schematic illustration of **a** pure ZnO and **b** C (P) doped ZnO band structure

photoactivity. In order to clearly understand the effect of non-metal dopants on ZnO band-gap and band edges a schematic diagram has been shown in Fig. 6. The presence of isolated states of C ($2p$) or P ($3p$) above the VBM is responsible for the enhancement in the visible light photoactivity of ZnO. Moreover, the CBM and VBM of doped ZnO shifts downward as compared to pure ZnO, indicating high water oxidation property. Although, on high doping concentration these impurity energy level might form a recombination centre for electron–hole pair and can reduce the quantum yield for the PEC reaction. To circumvent the problem of recombination one can go for co-doping of these non-metals dopants in pure ZnO.

4 Conclusions

In summary, we have studied the electronic band structure of C (P) doped ZnO by first principle DFT calculations. Our studies reveal that the impurity band originating from C ($2p$) and P ($3p$) does not mix well with the O $2p$ orbital bands. Thus, there is no significant band gap narrowing driven by C or P. However, the absorption in visible light region is mainly attributed to the isolated impurity bands located above the valence band and below the conduction which occur due to these dopants. Non-metal dopants can serve as good candidate for doping in ZnO as compared to metals, but co-doping of non-metals can also be a viable alternative technique for further enhancing the PEC activity of ZnO.

Acknowledgments Financial assistance from CSIR-HRDG, Government of India, New Delhi is gratefully acknowledged. Dr. Vidhika Sharma is thankful to University Grants Commission, Government of India, New Delhi for Dr. D. S. Kothari Postdoc Fellowship and financial assistance. SP acknowledges J C Bose Fellowship grant towards completion of the work.

References

1. T.J. Jacobsson, V. Fjallstrom, M. Edoff, T. Edvinsson, *Energy Environ. Sci.* **7**, 2056–2070 (2014)

2. I. Dincer, C. Acar, *Int. J. Hydrogen Energ.* **40**, 11094–11111 (2015)
3. A. Fujishima, K. Honda, *Nature* **238**, 37–38 (1972)
4. T. Bak, J. Nowotny, M. Rekas, C.C. Sorrell, *Int. J. Hydrogen Energ.* **27**, 991–1022 (2002)
5. M. Najim, G. Modi, Y.K. Mishra, R. Adelung, D. Singh, V. Agarwala, *Phys. Chem. Chem. Phys.* **17**, 22923–22933 (2015)
6. Y.K. Mishra, S. Kaps, A. Schuchardt, I. Paulowicz, X. Jin, D. Gedamu, S. Freitag, M. Claus, S. Wille, A. Kovalev, S.N. Gorb, R. Adelung, *Part. Part. Syst. Charact.* **30**, 775–783 (2013)
7. J. Grottrup, I. Paulowicz, A. Schuchardt, V. Kaidas, S. Kaps, O. Lupan, R. Adelung, Y.K. Mishra, *Ceram. Int.* **42**, 8664–8676 (2016)
8. V. Cretu, V. Postica, A.K. Mishra, M. Hoppe, I. Tiginyanu, Y.K. Mishra, L. Chow, N.H. de Leeuw, R. Adelung, O. Lupan, *J. Mater. Chem. A* **4**, 6527–6539 (2016)
9. Y.K. Mishra, G. Modi, V. Cretu, V. Postica, O. Lupan, T. Reimer, I. Paulowicz, V. Hrkac, W. Benecke, L. Kienle, R. Adelung, *Appl. Mater. Interfaces* **7**, 14303–14316 (2015)
10. T. Reimer, I. Paulowicz, R. Roder, S. Kaps, O. Lupan, S. Chemnitz, W. Benecke, C. Ronning, R. Adelung, Y.K. Mishra, *Appl. Mater. Interfaces* **6**, 7806–7815 (2014)
11. S.S. Alias, A.A. Mohamad, *Synthesis of zinc oxide by sol-gel method for photoelectrochemical cell*, 1st edn. (Springer, Singapore, 2014), pp. 41–50
12. V. Sharma, P. Kumar, N. Singh, S. Upadhyay, V.R. Satsangi, S. Dass, R. Shrivastav, *Int. J. Hydrogen Energ.* **37**, 12138–12149 (2012)
13. V. Sharma, P. Kumar, J. Shrivastava, A. Solanki, V.R. Satsangi, S. Dass, R. Shrivastav, *J. Mater. Sci.* **46**, 3792–3801 (2011)
14. V. Sharma, P. Kumar, J. Shrivastava, A. Solanki, V.R. Satsangi, S. Dass, R. Shrivastav, *Int. J. Hydrogen Energ.* **36**, 4280–4290 (2011)
15. V. Sharma, M. Dixit, V.R. Satsangi, S. Dass, S. Pal, R. Shrivastav, *Int. J. Hydrogen Energ.* **39**, 3637–3648 (2014)
16. X. Yang, A. Wolcott, G. Wang, A. Sobo, R.C. Fitzmorris, F. Qian, J.Z. Zhang, Y. Li, *Nano Lett.* **9**, 2331–2336 (2009)
17. Y.Z. Zheng, X. Tao, Q. Hou, D.T. Wang, W.L. Zhou, J.F. Chen, *Chem. Mater.* **23**, 3–5 (2011)
18. O. Haibon, H.J. Feng, L. Cuiyan, C. Liyun, F. Jie, *Mater. Lett.* **111**, 217–220 (2013)
19. S. Yu, W. Zhang, L. Li, H. Dong, D. Xu, Y. Jin, *Appl. Surf. Sci.* **298**, 44–49 (2014)
20. A.S. Alshammari, L. Chi, X. Chen, A. Bagabas, D. Kramer, A. Alromaeh, Z. Jiang, *RSC Adv.* **5**, 27690–27698 (2015)
21. S. Liu, C. Li, J. Yu, Q. Xiang, *Cryst. Eng. Comm.* **13**, 2533–2541 (2011)
22. X.H. Pan, J. Jiang, Y.J. Zeng, H.P. He, L.P. Zhu, Z.Z. Ye, B.H. Zhao, X.Q. Pan, *J. Appl. Phys.* **103**, 023708-4 (2008)
23. L. Franklin, C.E. Ekuma, G.L. Zhao, D. Bagayoko, *J. Phys. Chem. Solids* **74**, 729–736 (2013)
24. H.J. Kulik, M. Cococcioni, D.A. Scherlis, N. Marzari, *Phys. Rev. Lett.* **97**, 103001–103004 (2006)
25. W. Yu, J. Zhang, T. Peng, *Appl. Catal. B* **181**, 220–227 (2016)
26. L. Guan, B. Liu, Q. Li, Y. Zhou, J. Guo, G. Jia, Q. Zhao, Y. Wang, G. Fu, *Phys. Lett. A* **375**, 939–945 (2011)
27. G.S. Algharndi, A.Z. Alzahrani, *Phys. B* **407**, 3975–3981 (2012)
28. Y.W. Heo, S.J. Park, K. Ip, S.J. Pearton, D.P. Norton, *Appl. Phys. Lett.* **83**, 1128–1130 (2003)